

Accepted Manuscript

Design, synthesis and biological evaluation of 4- aniline-thieno[2,3-*d*]pyrimidine derivatives as MNK1 inhibitors against renal cell carcinoma and nasopharyngeal carcinoma

Min Zhang, Li Jiang, Jia Tao, Zhaoping Pan, Mingyao He, Dongyuan Su, Gu He, Qinglin Jiang

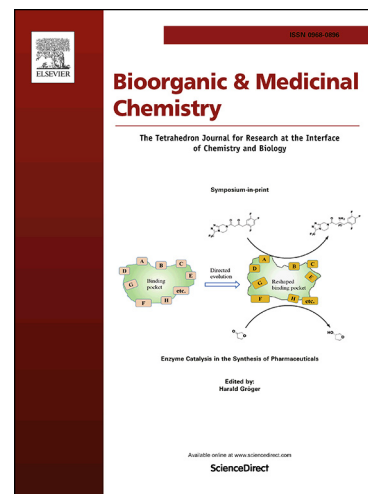
PII: S0968-0896(19)30439-0
DOI: <https://doi.org/10.1016/j.bmc.2019.04.022>
Reference: BMC 14876

To appear in: *Bioorganic & Medicinal Chemistry*

Received Date: 18 March 2019
Revised Date: 10 April 2019
Accepted Date: 14 April 2019

Please cite this article as: Zhang, M., Jiang, L., Tao, J., Pan, Z., He, M., Su, D., He, G., Jiang, Q., Design, synthesis and biological evaluation of 4- aniline-thieno[2,3-*d*]pyrimidine derivatives as MNK1 inhibitors against renal cell carcinoma and nasopharyngeal carcinoma, *Bioorganic & Medicinal Chemistry* (2019), doi: <https://doi.org/10.1016/j.bmc.2019.04.022>

This is a PDF file of an unedited manuscript that has been accepted for publication. As a service to our customers we are providing this early version of the manuscript. The manuscript will undergo copyediting, typesetting, and review of the resulting proof before it is published in its final form. Please note that during the production process errors may be discovered which could affect the content, and all legal disclaimers that apply to the journal pertain.



Design, synthesis and biological evaluation of 4-aniline-thieno[2,3-*d*]pyrimidine derivatives as MNK1 inhibitors against renal cell carcinoma and nasopharyngeal carcinoma

Min Zhang,^{†,1} Li Jiang,^{†,1} Jia Tao,¹ Zhaoping Pan,² Mingyao He,² Dongyuan Su,³

Gu He^{2,} and Qinglin Jiang^{1,*}*

¹ School of Pharmacy, Chengdu Medical College, Chengdu 610500, China.

² State Key Laboratory of Biotherapy and Cancer Center, West China Hospital, West China Medical School, Sichuan University and Collaborative Innovation Center for Biotherapy, Chengdu 610041, China.

³ Department of Gastroenterology, Chongzhou People's Hospital, Chengdu 611230, China

[†] These authors contributed equally.

* Corresponding authors: Prof. Qinglin Jiang: jql_cmc@163.com; Prof. Gu He: hegu@scu.edu.cn

ABSTRACT: MAP Kinase Interacting Serine/Threonine Kinase 1 (MNK1) play important roles in the signaling transduction of MAPK pathways. It is significantly overexpressed in renal clear cell carcinoma and head-neck squamous cell carcinoma tissues in both mRNA and protein levels. Based on the crystallographic structure of MNK1 protein and binding modes analysis of known MNK inhibitors, we have designed and synthesized a series of 4-aniline-thieno[2,3-d]pyrimidine derivatives as potential MNK1 inhibitors. These synthetic compounds are tested in biochemical and cell proliferation assays, and six of them display potent inhibitory capacity against MNK1 kinase and cancer cell lines. Compound **12dj** with strongest inhibitory capacity is transferred to molecular mechanism studies, and the results indicated that **12dj** remarkably suppresses the phosphorylation of EIF4E, a substrate of MNK1. And the expression levels of MNK1, ERK1/2 and pERK1/2 are not affected by compound **12dj** incubation in SUNE-1 and 786-O cells. In summary, our works suggested that these novel 4-aniline-thieno[2,3-d]pyrimidine based MNK1 inhibitors might be attractive lead compounds for targeted therapy of renal cell carcinoma and nasopharyngeal carcinoma.

Keywords: MNK; thieno[2,3-d]pyrimidine; apoptosis; renal cell carcinoma; nasopharyngeal carcinoma.

1. Introduction

The MAPK-interacting kinases (MNKs, including MNK1 and MNK2) is belong to a serine/threonine protein kinases family that are phosphorylated and activated by MAPK pathways such as ERK1/2 or p38 MAPK and downstream regulating translation initiator complexes by phosphorylating the eukaryotic initiation factor 4E (eIF4E).[1-6] The oncogenic roles of MNKs and eIF4E had been reported in several types of malignances, including breast cancer, Castrate-resistant Prostate Cancer, hepatocellular carcinoma and lymphoma, etc.[7-13] We analyzed the MNK1 mRNA and protein expression profiles in the Cancer Genome Atlas (TCGA)[14, 15] and ProteinAtlas database[16], respectively (Figure 1).

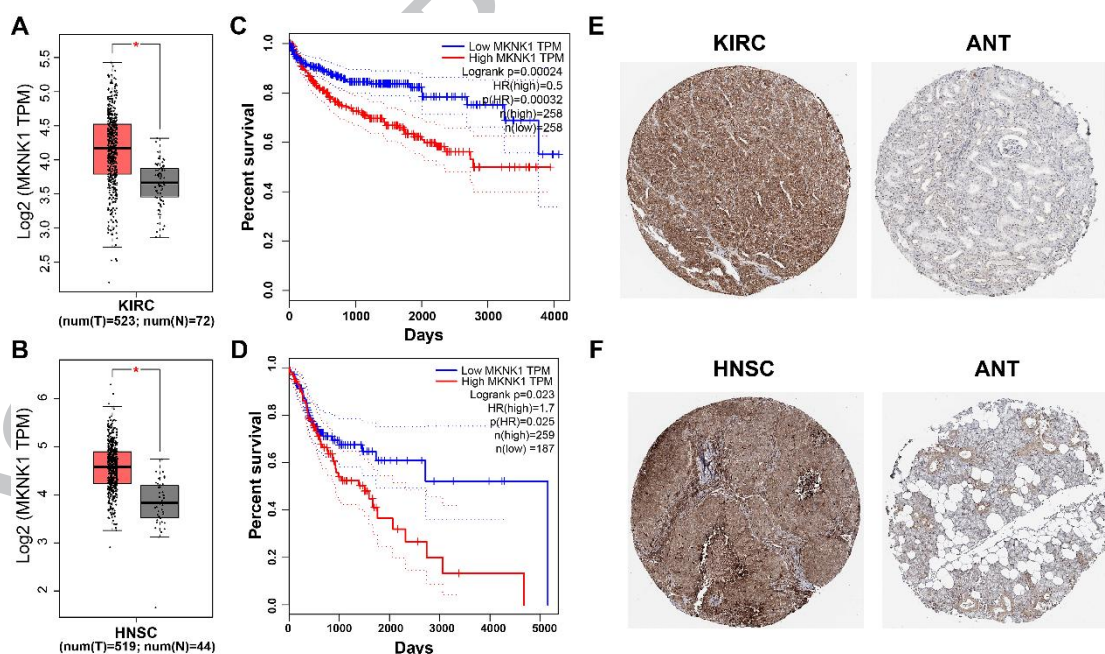


Figure 1. The mRNA and protein expression levels of MNK1 in KIRC and HNSC. (A and B) The boxplot of MNK1 expression in KIRC and HNSC cohort retrieved from TCGA database, respectively (*, $p < 0.05$); (C and D) The survival curves of KIRC and HNSC patients differed by the median expression levels of MNK1; (E and F) The protein expression levels of MNK1 determined by IHC in KIRC and HNSC tissues, retrieved from ProteinAtlas database.

The results suggest MNK1 is significantly overexpressed at the mRNA and protein levels in patients with renal cell carcinoma (KIRC) or head-neck squamous cell carcinoma (HNSC).[17] Moreover, the patient with higher MNK1 expression is suffered the worse prognosis in KIRC and HNSC, respectively. In the past years, there were several series of MNKs inhibitors reported with diverse chemical scaffold, such as pyrazolo[3,4-d]pyrimidin derivative CGP57380[18-20] and dibenzofuran derivatives cercosporamide (see Figure 2),[21-23] which displayed MNKs inhibitory capacities at micromolar levels but also demonstrated strong inhibition on the off-target kinases. The imidazopyridine based inhibitor eFT508 exerted nanomolar inhibitory capacity on MNK1 and MNK2 without obvious effects on p38, JNK1, ERK1/2 and Src, etc.[24] Moreover, a multi-kinase inhibitor merestinib, which had entered to phase I clinical trials against leukemia and solid tumors, also displayed potent inhibition activity to MNKs.[25-27] In addition, an indazol-6-yl-pyridinone based inhibitor SEL-201 was reported inhibitory capacities on MNKs, the proliferation and metastasis of melanoma both in vitro and in vivo.[28] Recently, Jin et al. reported a series of novel MNKs inhibitors with thieno[2,3-d]pyrimidine scaffold, inhibiting the proliferation of cancer cells as well as the high-fat feed induced.[29]

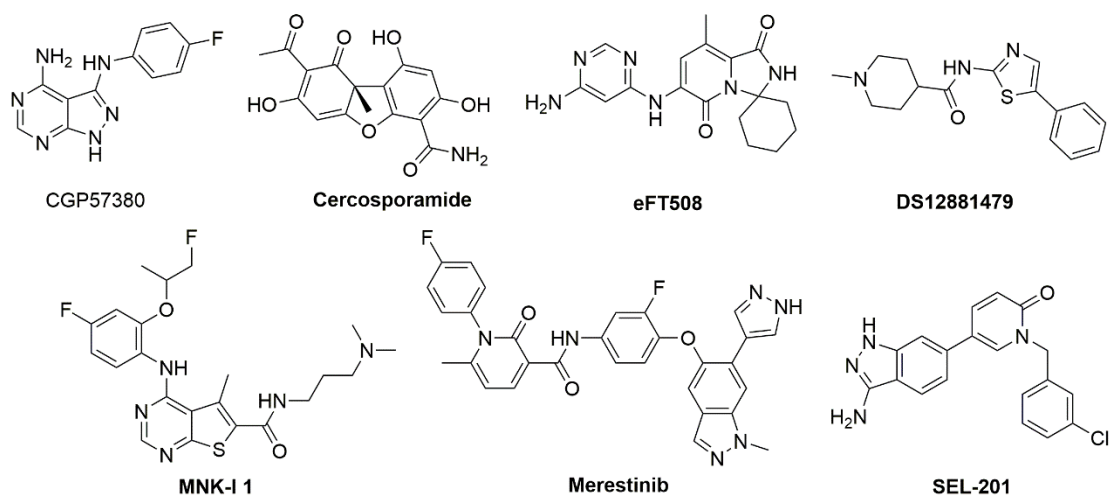


Figure 2. Chemical structures of structurally diverse MNK inhibitors.

Based on our previous works on the pyrido-thieno[2,3-d]pyrimidine based orally available kinase inhibitor with both inhibitory potency and good selectivity,[29] in the current manuscript, we have designed and synthesized a panel of potential MNK1 inhibitors, which showed promising cytotoxicity and apoptosis-inducing capacity against renal cell carcinoma and nasopharyngeal carcinoma cells. In particular, compound **12dj** exerts strongest MNK1 inhibitory capacity, and it is transferred to molecular mechanism studies, and the results indicate that **12dj** remarkably suppresses the phosphorylation of EIF4E, a substrate of MNK1. And the expression levels of MNK1, ERK1/2 and pERK1/2 are not affected by compound **12dj** incubation in SUNE-1 and 786-O cells. In brief, our works suggest that these novel 4-aniline-thieno[2,3-d]pyrimidine based MNK1 inhibitors might be attractive lead compounds for targeted therapy of renal cell carcinoma and nasopharyngeal carcinoma.

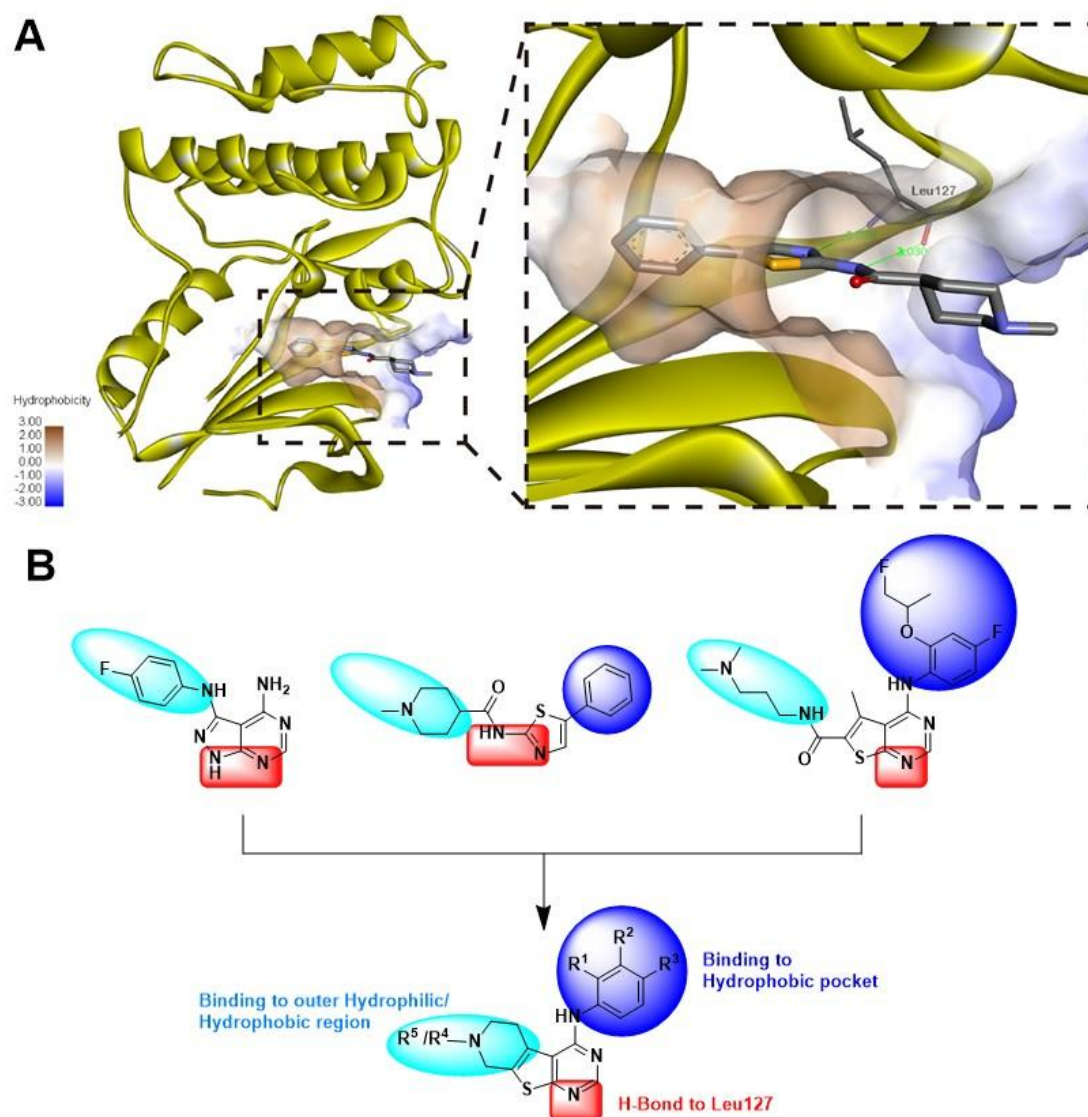


Figure 3. (A) Typical binding model of inhibitors to MNK1, DS12881479 was utilized as a representative inhibitor; (B) Strategy for the design of novel MNK1 inhibitors.

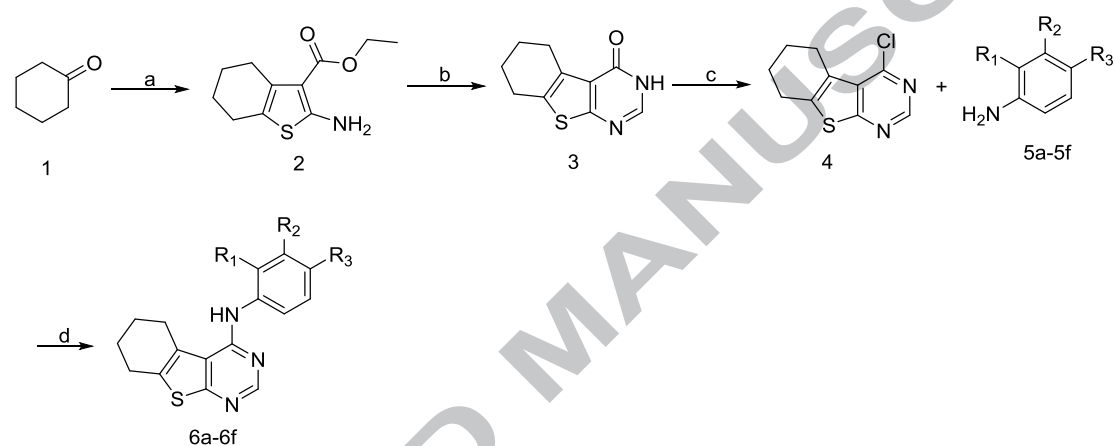
2. Results and discussion

2.1 Design and synthesis of novel MNK1 inhibitors

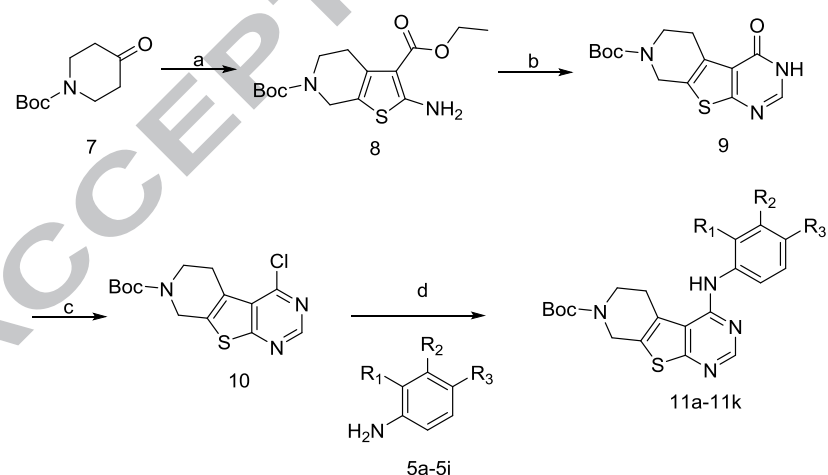
The binding modes of MNK1 to its inhibitors were visualized in Figure 3A, by using the co-crystallized structures of MNK1 and DS12881479 (PDB No. 5WVD).[30] The ligand binding pocket of MNK1 was comprised of an inner hydrophobic pocket and an outer hydrophilic region. Moreover, the hydrogen bonds between Leu127 and inhibitors were crucial to maintain binding affinities (Figure 3A). After compared the

structures of known MNK1 inhibitors, we found that there were three main fragments: a hydrophobic fragment to the inner hydrophobic pocket, the hydrogen donor/acceptor to Leu127 residue and a hydrophilic or hydrophobic fragment to bind the outer region. Therefore, a series of novel MNK1 inhibitors were designed based on a pyridothieno[2,3-d]pyrimidine scaffold (Figure 3B).

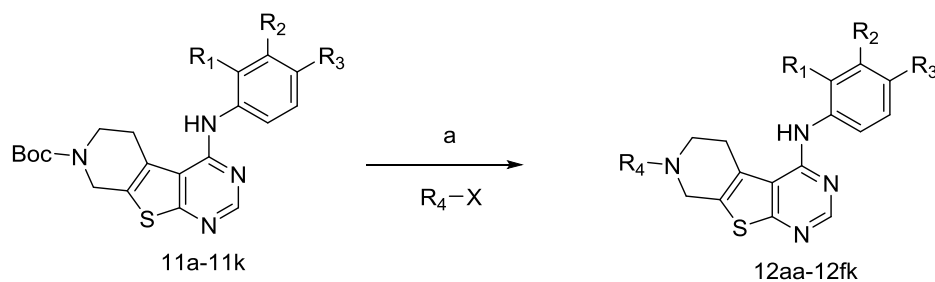
Scheme 1. Synthesis of Compounds 6a-6f, 11a-11k, 12a-12v, 13aa-13dk.



Reagents and conditions: a. NCCH₂CO₂Et, S₈, Et₃N, EtOH, reflux, 12h; b. formamidine acetate, DMF, 100°C, 16h; c. SOCl₂, reflux, 4h; d. NaH, 1,4-dioxane, 90°C, 2 hours.



Reagents and conditions: a. NCCH₂CO₂Et, S₈, Et₃N, EtOH, reflux, 12h; b. formamidine acetate, DMF, 100°C, 16h; c. SOCl₂, reflux, 4h; d. NaH, 1,4-dioxane, 90°C, 2 hours.



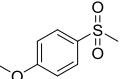
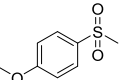
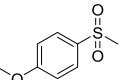
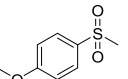
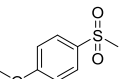
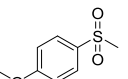
Reagents and conditions: a. 9N HCl, ethylacetate, 25°C, 30 min and then Et₃N, THF, rt, 4 hours.

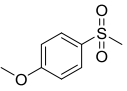
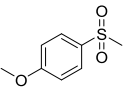
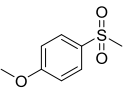
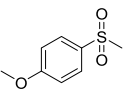
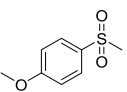
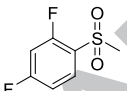
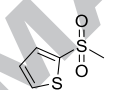
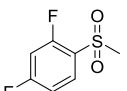
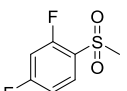
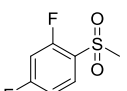
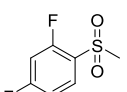
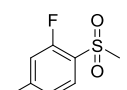
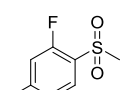
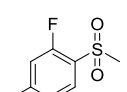
The synthesis route of compounds **6a-6f**, **11a-11k** and **12aa-12fk** were shown in **Scheme 1**. In general, for the preparation of the **6a-11a** and **12aa**, we chose cyclohexanone and N-Boc-4-piperidone as the starting materials respectively with ethyl cyanoacetate and sulfur to obtain **2** and **8** in yield 76% and 87%, the compound **2** and **8** was respectively reacted with formamidine acetate in DMF for 12h at 100°C to give **3** and **9** in yield 91% and 90%, the compound **3** and **9** was converted to **4** and **10** by treatment with SOCl₂ in yield 70% and 73%, the compound **4** was reacted with **5a** in 2-propanol at 100°C to give **6a** in yield 73%, meanwhile the compound **9** was reacted with **5a** and NaH in anhydrous 1,4-dioxane to give **11a** in yield 53%, Finally, the benzyl group of **11a** was removed by 9N HCl, the obtained compound was treated with iodomethane in THF to give **12aa** in yield 49%. The synthesized target compounds and key intermediates were characterized by ¹H NMR, ¹³C NMR and HR-MS (high-resolution mass spectrometry), the detailed experimental procedures and characterization were presented in experimental sections.

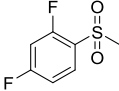
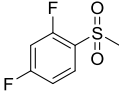
Table 1. Evaluations of compounds Compounds **6a-6f**, **11a-11k** and **12aa-12fk**.

No.	R1	R2	R3	R4	MNK1 IC ₅₀ (μ M) ^a	Cell Viability(%) ^{b,c}	
						SUNE-1	786-O
6a	H	F	H	-	2.18	68.08	71.20
6b	H	Cl	H	-	2.43	66.16	77.60
6c	H	H	Cl	-	1.62	59.39	68.00
6d	H	OCH ₃	H	-	1.70	62.19	76.80
6e	H	CH ₃	H	-	1.79	66.98	75.20
6f	H	H	Br	-	1.51	52.52	64.00
11a	H	F	H	-	2.19	71.42	76.00
11b	H	Cl	H	-	2.17	73.99	79.20
11c	H	H	Cl	-	2.24	65.80	77.60
11d	H	OCH ₃	H	-	1.95	71.35	79.20
11e	H	CH ₃	H	-	2.50	76.39	82.40
11f	H	H	Br	-	1.81	63.28	71.20
11g	F	H	F	-	1.62	44.92	62.40
11h	Br	H	F	-	1.72	50.60	55.20
11i	F	H	Cl	-	2.16	53.94	59.20
11j	OCH ₃	H	F	-	1.34	38.77	53.60
11k	Br	H	CH ₃	-	1.70	57.85	60.80
12aa	H	F	H	CH ₃	2.04	65.18	72.00

12ab	H	Cl	H	CH ₃	1.87	66.91	72.00
12ac	H	H	Cl	CH ₃	1.82	53.65	59.20
12ad	H	OCH ₃	H	CH ₃	2.29	65.97	71.20
12ae	H	CH ₃	H	CH ₃	2.22	69.22	86.40
12af	H	H	Br	CH ₃	1.69	55.07	61.60
12ag	F	H	F	CH ₃	1.09	35.66	56.00
12ah	Br	H	F	CH ₃	1.47	38.81	54.40
12ai	F	H	Cl	CH ₃	1.85	47.79	66.40
12aj	OCH ₃	H	F	CH ₃	0.93	32.47	57.60
12ak	Br	H	CH ₃	CH ₃	1.65	45.83	57.60
12ba	H	F	H	Bn	2.08	58.84	64.00
12bb	H	Cl	H	Bn	2.29	64.75	68.00
12bc	H	H	Cl	Bn	1.54	48.16	66.40
12bd	H	OCH ₃	H	Bn	1.92	58.76	64.80
12be	H	CH ₃	H	Bn	2.11	67.33	76.80
12bf	H	H	Br	Bn	1.69	42.86	65.60
12bg	F	H	F	Bn	1.10	31.61	48.00
12bh	Br	H	F	Bn	1.12	39.86	56.00
12bi	F	H	Cl	Bn	1.31	45.72	60.80
12bj	OCH ₃	H	F	Bn	1.00	33.50	45.60

12bk	Br	H	CH ₃	Bn	1.57	50.11	66.40
12ca	H	F	H		1.99	62.13	78.50
12cb	H	Cl	H		1.64	56.07	68.86
12cc	H	H	Cl		1.65	41.83	56.66
12cd	H	OCH ₃	H		2.02	51.30	57.04
12ce	H	CH ₃	H		2.06	67.32	79.46
12cf	H	H	Br		1.25	33.60	50.08
12cg	F	H	F		1.08	28.52	42.82
12ch	Br	H	F		1.16	36.27	58.62
12ci	F	H	Cl		1.26	35.55	57.24
12cj	OCH ₃	H	F		1.10	29.37	44.30
12ck	Br	H	CH ₃		1.65	53.90	65.52
12da	H	F	H		1.39	48.46	62.77
12db	H	Cl	H		1.40	47.66	66.93
12dc	H	H	Cl		1.22	30.54	50.83
12dd	H	OCH ₃	H		2.14	56.43	69.14
12de	H	CH ₃	H		1.41	49.14	63.31
12df	H	H	Br		1.07	30.24	50.59

12dg	F	H	F		0.83	28.96	39.97
12dh	Br	H	F		1.00	34.02	53.61
12di	F	H	Cl		1.15	31.44	54.75
12dj	OCH ₃	H	F		0.65	21.20	36.96
12dk	Br	H	CH ₃		1.89	55.52	72.41
12ea	H	F	H		2.02	50.40	68.32
12eb	H	Cl	H		1.74	53.30	69.84
12ec	H	H	Cl		1.50	46.80	55.04
12ed	H	OCH ₃	H		1.88	59.85	72.68
12ee	H	CH ₃	H		2.40	68.00	76.00
12ef	H	H	Br		1.73	54.00	68.80
12eg	F	H	F		1.10	31.05	44.84
12eh	Br	H	F		1.28	36.10	56.88
12ei	F	H	Cl		1.54	40.42	61.94

12ej	OCH ₃	H	F		0.93	32.32	49.86
12ek	Br	H	CH ₃		1.68	49.45	62.76
12fa	H	F	H		1.50	48.89	56.71
12fb	H	Cl	H		1.38	50.64	58.91
12fc	H	H	Cl		1.63	45.25	66.60
12fd	H	OCH ₃	H		2.35	62.84	66.27
12fe	H	CH ₃	H		2.13	66.64	70.91
12ff	H	H	Br		1.39	44.28	66.62
12fg	F	H	F		1.46	37.82	57.45
12fh	Br	H	F		0.97	32.49	54.79
12fi	F	H	Cl		1.36	39.21	59.37
12fj	OCH ₃	H	F		0.94	28.89	42.31
12fk	Br	H	CH ₃		1.56	47.70	60.56
CGP-5 7380	-	-	-	-	2.74	57.48	61.35

^a IC₅₀ values were determined from KinaseProfiler of Eurofins. The data represent the mean values of two independent experiments.

^b Cells were incubated to 1.0 μM corresponding compound for 24 hours.

^b Each compound was tested in triplicate; the data are presented as the mean values.

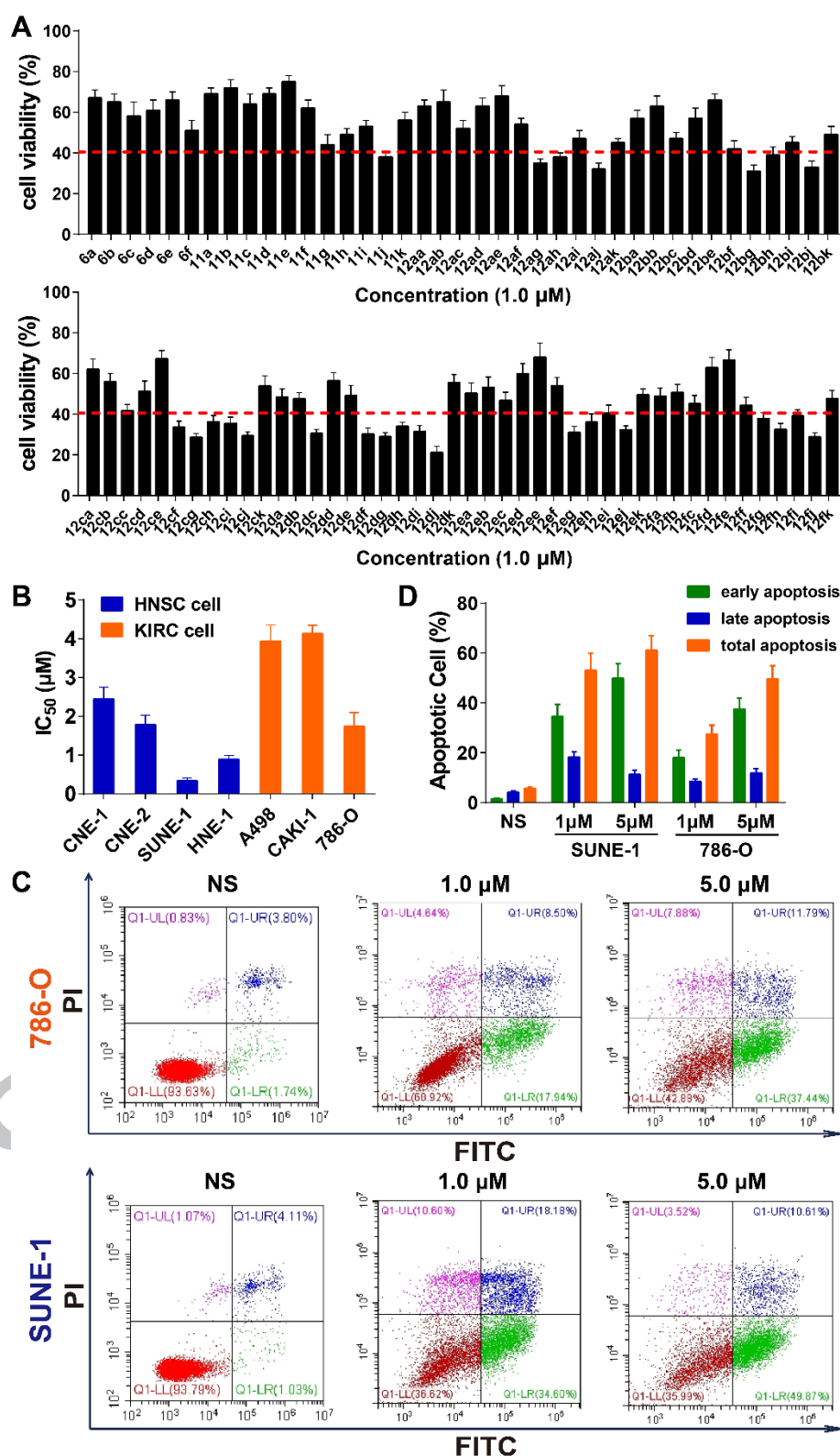


Figure 4. (A) Cytotoxicity of compounds **6a-f**, **11a-k**, **12aa-fk** against nasopharyngeal carcinoma cell lines SUNE-1 based on the MTT method; (B) IC₅₀ values of compound **12dj** against a panel of renal cell carcinoma and nasopharyngeal carcinoma cell lines;

(C) and (D) Apoptosis in SUNE-1 cells treated with compound **12dj** based on Annexin V/PI dual staining. Values are mean \pm SD (n = 3).

2.2 Novel MNK1 inhibitors possess good kinase inhibition and suppress cancer cells proliferation

We have evaluated the MNK1 kinase inhibitory capacities of compounds **6a-6f**, **11a-11k** and **12aa-12fk** by using a γ -[³²P]-ATP competitive inhibition assay. As positive control drugs, we used the known inhibitor CGP-57380. The IC₅₀ values for each compound were determined as the mean values of three duplicated experiments (Table 1). The inhibition rates on cell viability of SUNE-1 and 786-O cells for each compound at 1.0 μ M were determined were also measured by MTT method (Figure 4A and Table 1). Further structure-activity relationships investigation also revealed that the R1 and R3 substitution of 4-aniline fragment could be replaced by 2,4-di-F (12dg), 2-Br-4-F (12dh), 2-F-4-Cl (12di), 2-OCH₃-4-F (12dj) or 2-Br-4-CH₃ (12dk) with obviously increasing the MNK1 inhibitory potencies as well as cell proliferation inhibition. For the R4 substitution, the alkyl or benzyl substituted compounds 12aa-12bk exhibited moderate MNK1 inhibitory capacities, and the aromatic sulfonyl substituted compounds demonstrated better inhibitory potencies in both MNK1 and cell proliferation assays. When the R4 position of pyrido[4',3':4,5]thieno[2,3-d]pyrimidine ring substituted by a 4-methoxyphenyl sulfonyl group, the resulting compound 12dj was almost four times stronger potent than the lead molecule 6a. Compounds **12df-12dj** worked better than the other compounds by inhibiting the kinase activity of MNK1 as well as the proliferation of renal cell

carcinoma and nasopharyngeal carcinoma cell lines (Figure 4B). Among the more active compounds **12df-12dj**, compound **12dj** with a halogen at the 4-F,2-OMe-phenyl on the 4-position of thieno[2,3-d]pyrimidine scaffold demonstrated the greatest MNK1 inhibition and cytotoxicity. Compound **12dj** inhibited both the MNK1 kinase and cancer cell proliferation prior than known inhibitor CGP-57380. Moreover, compound **12dj** displayed submicromolar inhibition IC_{50} values on MNK1 kinase and SUNE-1 cell viability assays. Therefore, compound **12dj** was transferred to further molecular mechanism studies.

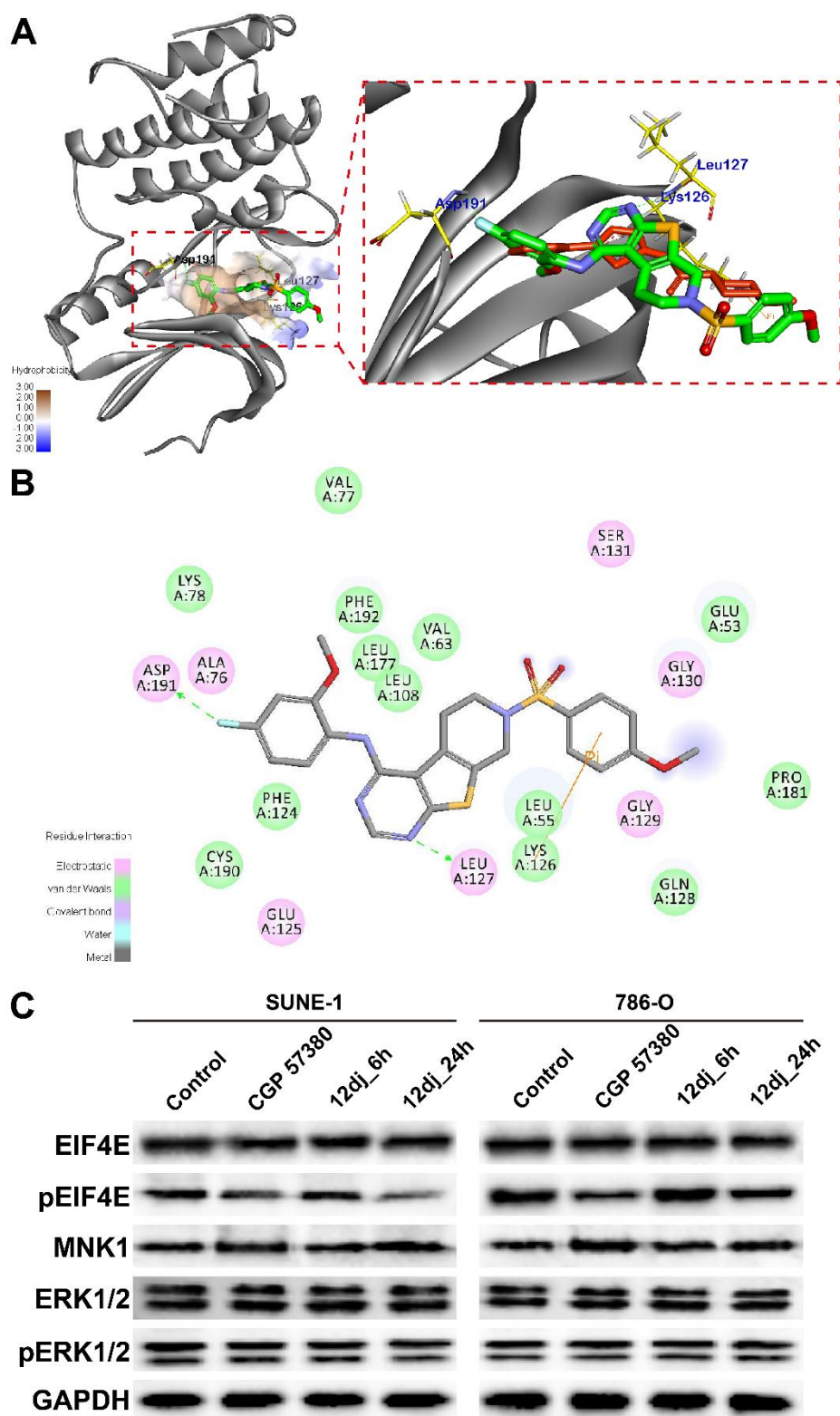


Figure 5. (A) Comparison of the binding modes of compound **12dj** (green) with the experimental conformation of DS12991479 (red) bound to MNK1 kinase domain; (B) Schematic depiction of the potential interaction modes of compound **12dj** in the ATP pocket of MNK1; (C) Western blotting analysis of MNK1, ERK1/2, eIF4E and their phosphorylated proteins in SUNE-1 and 786-O cells after 24-h incubation of 1 μ M CGP-57380, or 6h and 24-h incubation of 1 μ M compound **12dj**, respectively.

2.3 Novel MNK1 inhibitor **12dj** induces apoptosis without affects the expression and phosphorylation of ERK1/2

The apoptotic cell death of SUNE-1 and 786-O cells induced by compound **12dj** incubation were determined by the flowcytometry analysis with an Annexin V/PI dual staining kit (Figure 4C and 4D). According to Figure 4C-4D, the percentage of total apoptotic cells in the 5 μ M **12dj** treatment groups were raised from 5.7% to 61.1% in SUNE-1 cell and 49.6% in 786-O cell, respectively. In addition, the early apoptotic cells in 5 μ M **12dj** treated groups were remarkably higher than in the 1 μ M **12dj** treated groups for both cells. For the late apoptotic cells, there were no significant differences between the 1 μ M **12dj** treated groups and 5 μ M **12dj** treated groups. Above results suggested that the cytotoxicity of compound **12dj** possibly dependent on the apoptotic cell death subroutine with a concentration-dependent manner.[31-33]

The potential binding modes of compound **12dj** into the ATP pocket of MNK1 kinase domain was performed by CDOCKER molecular docking module in Accelrys Discovery Studio 2.5 software (Figure 5A). By comparison to the co-crystallized inhibitor DS12881470, compound **12dj** formed similar hydrogen bonds with Leu127, hydrophobic interaction to the inner residues such as Leu108, Phe124, Leu177 and Phe192. In addition, the possible hydrogen bond between the 4-F,2-OMe-phenyl fragment and Asp191, and the cation- π interaction between Lys126 and the 4-methoxybenzenesulfonamide fragment might enhanced the binding affinity of **12dj** to MNK1 kinase domain. The 2D-diagram of interactions between **12dj** and interactive residues were depicted into Figure 5B. To further verify the selectivity of

compound **12dj** to the ERK-MNK-eIF4E signaling axis, we determined its influence on the expression of ERK1/2, pERK1/2, MNK1 eIF4E and p-eIF4E in SUNE-1 and 786-O cells with the known MNK1 inhibitor CGP-57380 as a positive control (Figure 5C). As shown in Figure 5C, the **12dj** or CGP-57380 incubation for 24 hours selectively declined the phosphorylation of eIF4E in both cells, the phosphorylation of ERK1/2 and expression of total ERK1/2, MNK1 and eIF4E were not affected. Furthermore, the **12dj** induced inhibition of eIF4E phosphorylation, a MNK1 substrate, by a time-dependent manner. These results suggested that compound **12dj** could competitively suppress the MNK1 without interfere the upstream ERK1/2 functions. In addition, the inhibitory capacity of eIF4E phosphorylation of **12dj** in SUNE-1 cells was obviously stronger than that of 786-O cells, which might explain the cytotoxic difference in the renal cell carcinoma cells and nasopharyngeal carcinoma cells after **12dj** incubation.

3. Conclusions

In the current study, based on the rational drug design method, we have prepared, in good yield, a series of 4- aniline-pyridothieno[2,3-d]pyrimidine derivatives bearing various substituted groups. Structure-activity analysis of the prepared compounds afforded **12dj**, which showed strong ability to inhibit both MNK1 and a panel of cancer cell lines. The compound **12dj** also selectively suppressed the eIF4E phosphorylation and induced apoptosis in both SUNE-1 and 786-O cells. Taken together, these results suggested that these novel 4-aniline-thieno[2,3-d]pyrimidine based MNK1 inhibitors might be attractive lead compounds for targeted cancer

therapy, especially for nasopharyngeal carcinoma.

4. Experimental Section

4.1 Chemistry

The general synthesis procedures of representative compounds and intermediates were described bellowed, the detailed synthesis and characterization of all compounds, and the spectra of ^1H NMR, ^{13}C NMR and HR-MS were provide in the supplementary materials. [34-36]

General Procedures of Method for the Synthesis of 6a, 11a, 12aa, 12ca

Ethyl 2-amino-4,5,6,7-tetrahydrobenzo[*b*]thiophene-3-carboxylate (2). To a mixture of cyclohexanone(**1**)(9.80g, 100mmol) , ethyl cyanoacetate (11.32 g, 200.0 mmol), and sulfur (3.20 g, 100.0 mmol) in absolute ethanol (200 mL) was added triethylamine (20mL) and refluxed for 12 h; the reaction mixture was concentrated and the residue was partitioned between water and ethyl acetate. The organic layer was separated, and concentrated, and the crude product was recrystallized with ethanol (150ml), to give **2**. Yield 76%, light yellow crystal. ^1H NMR (400 MHz, Chloroform-*d*) δ 7.20 (s, 2H), 4.14 (q, $J = 7.2$ Hz, 2H), 2.59 (t, $J = 5.6$ Hz, 2H), 2.41 (t, $J = 5.6$ Hz, 2H), 1.74 – 1.58 (m, 4H), 1.24 (t, $J = 7.2$ Hz, 3H).

3,4,5,6,7,8-Hexahydrobenzo[4,5]thieno[2,3-*d*]pyrimidin-4-one(3). A mixture of (**2**) (4.50g, 20.0mmol)and formamidine acetate (3.12g, 30.0mmol)was sterred in DMF for 12 h at 100°C. The reaction mixture was cooled, water was added, and the precipitate formed was collected by filtration, and washed thoroughly with water to give **3**, Yield,

91%. ¹H NMR (400 MHz, Chloroform-*d*) δ 7.91(s,1H) , 3.02-2.99 (m,2H) , 2.79-2.76 (m, 2H) , 2.02-1.83 (m, 4H).

4-Chloro-5,6,7,8-tetrahydrobenzo[4,5]thieno[2,3-d]pyrimidine(4). A mixture of (3) (12.0g,58.2mmol), SOCl₂ (100mL)and DMF(2ml) was refluxed for 4 h. The reaction mixture was cooled in an ice bath and then carefully neutralized by the addition of aqueous sodium bicarbonate solution. The resulting mixture was extracted with ethyl acetate, the organic layer was separated, dried over MgSO₄, and concentrated, and the crude product was purified by silica gel column chromatography using a mixture of Petroleum ether: Dichloromethane (5:1), to give **4**, Yield, 70%. ¹H NMR (400 MHz, Chloroform-*d*) δ 8.69 (s, 1H), 3.10-3.07(m, 2H), 2.88-2.86 (m, 2H), 1.92-1.89 (m, 4H).

N-(3-fluorophenyl)-5,6,7,8-tetrahydrobenzo[4,5]thieno[2,3-d]pyrimidin-4-amine

(6a) A mixture of 3-fluoroaniline(**5a**)(333mg,3mmol) and 4-Chloro-5,6,7,8-tetrahydrobenzo[4,5]thieno[2,3-d]pyrimidine (**4**) (449 mg, 2mmol) and 2-propanol (15 mL) in sealed tube was stirred for 6 h at 100°C. The reaction mixture was concentrated, and the residue was partitioned between water and dichloromethane. The organic layer was washed with water, dried over MgSO₄, and concentrated. The crude product was purified by silica gel column chromatography using a mixture of hexane: ethyl acetate (6:1) to give **6a**. Yield 73%, White powder, m. p. 114.5 – 116.3°C. ¹H NMR (400 MHz, Chloroform-*d*) δ 8.52 (s, 1H), 7.75 (dt, J = 11.1, 2.3 Hz, 1H), 7.33 – 7.17 (m, 3H), 6.92 – 6.68 (m, 1H), 3.07 (tt, J = 6.0, 3.1 Hz, 2H), 2.87 (tt, J = 6.0, 3.1Hz, 2H), 2.11 – 1.86 (m, 4H). ¹³C NMR (100 MHz,

Chloroform-*d*) δ 166.52, 163.09(d, J = 244 Hz, 1C), 154.26, 152.34, 140.21(d, J = 11 Hz, 1C), 135.22, 130.00(d, J = 9 Hz, 1C), 124.50, 116.77, 115.91 (d, J = 3 Hz, 1C), 110.32(d, J = 22 Hz, 1C), 108.24(d, J = 27 Hz, 1C), 26.53, 25.57, 22.56, 22.39 .
 HRMS(ESI) calcd for $C_{16}H_{15}FN_3S^+$ $[M+H]^+$ 300.0965, found 300.0966.

6-(tert-butyl) 3-ethyl

2-amino-4,7-dihydrothieno[2,3-*c*]pyridine-3,6(5H)-dicarboxylate(8).

Compound(8) was synthesized from N-Boc-4-piperidone (7), in a manner similar to(2), after stirring for 16 h at room temperature, the precipitate was collected by filtration and washed with ethanol to give 87% yield, white powder, 1H NMR (400 MHz, Chloroform-*d*) δ 6.02 (s, 2H), 4.35 (s, 2H), 4.26 (q, J = 7.0 Hz, 2H), 3.61 (t, J = 5.7 Hz, 2H), 2.80 (t, J = 5.7 Hz, 2H), 1.48 (s, 9H), 1.34 (t, J = 7.0 Hz, 3H).

tert-butyl

4-oxo-3,5,6,8-tetrahydropyrido[4',3':4,5]thieno[2,3-*d*]pyrimidine-7(4H)-carboxyl

ate(9). Compound (9) was synthesized from compound(8) and formamidine acetate, in a manner similar to (9), Yield, 90%, light yellow powder, 1H NMR (400 MHz, Chloroform-*d*) δ 11.99 (s, 1H), 7.99 (s, 1H), 4.66 (s, 2H), 3.74 (t, J = 5.8 Hz, 2H), 3.13 (t, J = 5.8 Hz, 2H), 1.50 (s, 9H).

tert-butyl

4-chloro-5,8-dihydropyrido[4',3':4,5]thieno[2,3-*d*]pyrimidine-7(6H)-carboxylate(

10). Compound (10) was synthesized from compound(9) and $SOCl_2$, in a manner

similar to (4), Yield, 73%, white powder, ^1H NMR (400 MHz, Chloroform-*d*) δ 8.77 (s, 1H), 4.74 (s, 2H), 3.80 (t, $J = 5.8$ Hz, 2H), 3.21 (t, $J = 5.8$ Hz, 2H), 1.51 (s, 9H).

tert-butyl4-((3-fluorophenyl)amino)-5,8-dihydropyrido[4',3':4,5]thieno[2,3-d]pyrimidine-7(6H)-carboxylate (11a). To a suspension of 60% NaH(120mg, 3mmol) in anhydrous 1,4-dioxane(10ml) was added a solution of 3-fluoroaniline(5a) (222mg, 2mmol) in anhydrous 1,4-dioxane(5ml), the reaction mixture was stirred for 20 min at room temperature and then compound(10)(325mg, 1mmol) in 1,4-dioxane(5ml) was added to the above reaction mixture, the mixture was stirred for another 2 hours at 90°C, at the end of the reaction, the excessive NaH was quenched by H₂O, the mixture was concentrated and the residue was partitioned between water and ethyl acetate. The organic layer was separated, and concentrated, and then the crude product was purified by silica gel column chromatography using a mixture solvent of petroleum ether: ethylacetate (15:1), to give **11a**. Yield 53%, Light yellow powder, m. p. 164.4 – 165.0°C. ^1H NMR (400 MHz, Chloroform-*d*) δ 8.55 (s, 1H), 7.73 (d, $J = 11.0$ Hz, 1H), 7.32 (td, $J = 8.1, 6.3$ Hz, 1H), 7.23 (d, $J = 8.3$ Hz, 1H), 7.03 (s, 1H), 6.83 (tdd, $J = 8.2, 2.5, 1.0$ Hz, 1H), 4.72 (s, 2H), 3.86 (t, $J = 5.7$ Hz, 2H), 3.14 (t, $J = 5.7$ Hz, 2H), 1.51 (s, 9H). ^{13}C NMR (100 MHz, Chloroform-*d*) δ 167.00, 163.04 (d, $J = 243$ Hz, 1C), 154.64, 154.33, 152.81, 139.85 (d, $J = 11$ Hz, 1C), 130.07 (d, $J = 9$ Hz, 1C), 116.13, 116.07 (d, $J = 3$ Hz, 1C), 110.65 (d, $J = 21$ Hz, 1C), 108.42 (d, $J = 23$ Hz, 1C), 80.83, 28.41 (3C), 26.45. HRMS(ESI) calcd for C₂₀H₂₂FN₄O₂S⁺[M+H]⁺ 401.1442, found 401.1441.

N-(3-fluorophenyl)-7-methyl-5,6,7,8-tetrahydropyrido[4',3':4,5]thieno[2,3-d]pyrimidin-4-amine (12aa). Compound 11a (800mg, 2.0mmol) was dissolved in 10ml ethyl acetate and then 9N HCl (5ml) was added, the reaction mixture was stirred for 30 min at room temperature, the reaction solvent was neutralized by NaHCO₃ to pH=8, 50ml ethyl acetate and 30ml H₂O was added, after stirred adequately, the organic layer was separated, and concentrated, and then the crude product was purified by silica gel column chromatography using a mixture solvent of dichloromethane: methanol (20:1), to give white powder (540mg); Above white powder (150mg, 0.5mmol) was dissolved in THF (10ml), iodomethane(107mg, 0.75mmol) and triethylamine(0.5ml) were added in the solvent. after the reaction mixture was stirred for 1 hour at room temperature, the solvent was concentrated, the residues was purified by silica gel column chromatography using a mixture solvent of dichloromethane: methanol (40:1), to give (12aa) Yield 49%, White powder, m. p. 116.7 – 118.5°C. ¹H NMR (400 MHz, Chloroform-*d*) δ 8.54 (s, 1H), 7.75 (dt, *J* = 11.1, 2.3 Hz, 1H), 7.31 (td, *J* = 8.1, 6.2 Hz, 1H), 7.26 – 7.22 (m, 1H), 7.08 (s, 1H), 6.82 (tdd, *J* = 8.2, 2.5, 1.1 Hz, 1H), 3.72 (t, *J* = 1.9 Hz, 2H), 3.17 (tt, *J* = 5.7, 1.9 Hz, 2H), 2.90 (t, *J* = 5.7 Hz, 2H), 2.54 (s, 3H). ¹³C NMR (100 MHz, Chloroform-*d*) δ 166.85, 163.09 (d, *J*=243Hz, 1C), 154.65, 152.68, 140.04 (d, *J*=11Hz, 1C), 132.49, 130.06 (d, *J*=9Hz, 1C), 122.76, 116.18, 116.02 (d, *J*=3Hz, 1C), 110.54 (d, *J*=21Hz, 1C), 108.38 (d, *J*=27Hz, 1C), 54.03, 51.66, 45.33, 26.75. HRMS(ESI) calcd for C₁₆H₁₆FN₄S⁺ [M+H]⁺ 315.1074, found 315.1079.

N-(3-fluorophenyl)-7-((2-nitrophenyl)sulfonyl)-5,6,7,8-tetrahydropyrido[4',3':4,5]thieno[2,3-d]pyrimidin-4-amine (12ca). Compound (12ca) was synthesized from compound (11a) and 2-nitrobenzenesulfonyl chloride, in a manner similar to (12aa). Yield 88%, White powder, m. p. 212.2 – 212.8°C. ¹H NMR (400 MHz, DMSO-*d*₆) δ 8.49 (s, 1H), 8.40 (s, 1H), 8.15 (dd, *J* = 7.7, 1.5 Hz, 1H), 8.03 (dd, *J* = 7.8, 1.5 Hz, 1H), 7.95 – 7.86 (m, 2H), 7.63 (dt, *J* = 11.7, 2.3 Hz, 1H), 7.48 – 7.32 (m, 2H), 6.91 (td, *J* = 8.4, 2.5 Hz, 1H), 4.70 (s, 2H), 3.72 (t, *J* = 5.7 Hz, 2H), 3.34 (t, *J* = 5.7 Hz, 2H). ¹³C NMR (100 MHz, DMSO-*d*₆) δ 167.16, 162.50 (d, *J* = 240 Hz, 1C), 155.14, 153.08, 148.09, 141.46 (d, *J* = 11 Hz, 1C), 135.40, 133.11, 130.96, 130.73, 130.39 (d, *J* = 11 Hz, 1C), 128.68, 125.73, 124.96, 118.02 (d, *J* = 3 Hz, 1C), 116.82, 110.12 (d, *J* = 21 Hz, 1C), 108.97 (d, *J* = 26 Hz, 1C), 45.29, 43.16, 26.30. HRMS(ESI) calcd for C₂₁H₁₇FN₅O₄S₂⁺[M+H]⁺ 486.0701, found 486.0698.

4.2 Molecular docking.

The molecular docking analysis was performed by the CDocker module in the Accelrys Discovery Studio 2.5 software packages (BIOVIA, San Diego, CA, USA). The initial co-crystallized structure of MNK1 (PDB No. 5WVD) was retrieved from the Protein Data Bank (<http://www.rcsb.org>). All the computational parameters were used default settings without individual descriptions.[37-39]

4.3 Kinase inhibition assay of MNK1.

The kinase inhibition assay of MNK1 was provided by Eurofins Co. Ltd. with the KinaseProfiler services. The detailed experimental procedures had been described in our previous reports.[39-41]

4.4 Cell viability and apoptosis assays.

The cell viability assays of screened compounds were performed in SUNE-1 and 786-O cells, respectively with a constant concentration of 1 μ M and 24-hour incubation. The IC₅₀ values of compound **12dj** on a panel of renal cell carcinoma and nasopharyngeal carcinoma cells were performed on a series of concentration gradient with 8-10 points. The detailed experimental procedures had been described in our previous reports. And the known MNK1 inhibitor CGP-57380 was utilized as a positive control. Apoptosis assay of compound **12dj** was carried out by a BD FACSCalibur Flow Cytometer on SUNE-1 and 786-O cells, respectively. The detailed experimental procedures had been described in our previous reports.[42-44]

4.5 Western blot analysis

The primary antibodies of ERK1/2, pERK1/2, MNK1, eIF4E and p-eIF4E were obtained from Cell Signaling Technology (Danvers, MA, USA). After treatment by the procedures according to the figure legends, SUNE-1 or 786-O cells were harvested, trypsin digested and then washed twice by cold PBS. After lysated by RIPA buffer (Invitrogen, CA, USA) on ice, the cellular lysate was sonication denaturation and then cold centrifuged at 10000+ g for 30 min. The supernatant was collected, quantified the total protein concentration, and then separated by a SDS-PAGE electrophoresis, electro-transferred into a PVDF membrane, incubated by the corresponding primary

and secondary antibodies, and then visualized by an ECL (enhanced chemiluminescence) Kit.

Acknowledgements. We are grateful for financial support from the National Natural Science Foundation of China (21772131), the Fundamental Research Funds of Science & Technology Department of Sichuan Province (2017JY0123 and 19SYXHZ015), the Fundamental Research Funds for the Central Universities and Distinguished Young Scholars of Sichuan University (2015SCU04A13), the China Postdoctoral Science Foundation and the Open Research Fund from State Key Laboratory of Breeding Base of Systematic Research, Development and Utilization of Chinese Medicine Resources. The ^1H NMR and ^{13}C NMR spectrum were supplied as Supporting Information. This material is available free of charge via the Internet.

Competing interests. The authors declare no competing interests.

REFERENCES

- [1] J.E. Beggs, S.Y. Tian, G.G. Jones, J.L. Xie, V. Iadevaia, V. Jenei, G. Thomas, C.G. Proud, The MAP kinase-interacting kinases regulate cell migration, vimentin expression and eIF4E/CYFIP1 binding, *Biochemical Journal*, 467 (2015) 63-76.
- [2] C.R. Bramham, K.B. Jensen, C.G. Proud, Tuning Specific Translation in Cancer Metastasis and Synaptic Memory: Control at the MNK-eIF4E Axis, *Trends in Biochemical Sciences*, 41 (2016) 847-858.
- [3] M. Buxade, J.L. Parra, S. Rousseau, N. Shpiro, R. Marquez, N. Morrice, J. Bain, E. Espel, C.G. Proud, The Mnk1s are novel components in the control of TNF alpha biosynthesis and phosphorylate and regulate hnRNP A1, *Immunity*, 23 (2005) 177-189.
- [4] C.G. Proud, Mnk1s, eIF4E phosphorylation and cancer, *Biochimica Et Biophysica Acta-Genes and Cell Signaling*, 1849 (2015) 766-773.
- [5] G.C. Schepers, C.G. Proud, Does phosphorylation of the cap-binding protein eIF4E play a role in translation initiation?, *European Journal of Biochemistry*, 269 (2002) 5350-5359.
- [6] X.M. Wang, A. Flynn, A.J. Waskiewicz, B.L.J. Webb, R.G. Vries, I.A. Baines, J.A. Cooper, C.G. Proud, The phosphorylation of eukaryotic initiation factor eIF4E in response to phorbol esters, cell stresses, and cytokines is mediated by distinct MAP kinase pathways, *Journal of Biological Chemistry*, 273 (1998) 9373-9377.

- [7] N. Hay, Mnk earmarks eIF4E for cancer therapy, *Proceedings of the National Academy of Sciences of the United States of America*, 107 (2010) 13975-13976.
- [8] E.M. Kosciuczuk, D. Saleiro, L.C. Plataniias, Dual targeting of eIF4E by blocking MNK and mTOR pathways in leukemia, *Cytokine*, 89 (2017) 116-121.
- [9] A.K. Kwegyir-Afful, R.D. Bruno, P. Purushottamachar, F.N. Murigi, V.C. Njar, Galeterone and VNPT55 disrupt Mnk-eIF4E to inhibit prostate cancer cell migration and invasion, *The FEBS journal*, 283 (2016) 3898-3918.
- [10] S. Liu, J. Zha, M. Lei, Inhibiting ERK/Mnk/eIF4E broadly sensitizes ovarian cancer response to chemotherapy, *Clinical & translational oncology : official publication of the Federation of Spanish Oncology Societies and of the National Cancer Institute of Mexico*, 20 (2018) 374-381.
- [11] T.N.D. Pham, K. Kumar, B.T. DeCant, M. Shang, S.Z. Munshi, M. Matsangou, K. Ebine, H.G. Munshi, Induction of MNK Kinase-dependent eIF4E Phosphorylation by Inhibitors Targeting BET Proteins Limits Efficacy of BET Inhibitors, *Molecular cancer therapeutics*, 18 (2019) 235-244.
- [12] R.L. Silva, H.G. Wendel, MNK, EIF4E and targeting translation for therapy, *Cell cycle*, 7 (2008) 553-555.
- [13] F. Wu, S. Li, N. Zhang, W. Huang, X. Li, M. Wang, D. Bai, B. Han, Hispidulin alleviates high-glucose-induced podocyte injury by regulating protective autophagy, *Biomedicine & pharmacotherapy = Biomedecine & pharmacotherapie*, 104 (2018) 307-314.
- [14] M.S. Cline, B. Craft, T. Swatloski, M. Goldman, S. Ma, D. Haussler, J. Zhu, Exploring TCGA Pan-Cancer data at the UCSC Cancer Genomics Browser, *Scientific reports*, 3 (2013) 2652.
- [15] H.S. Kim, J.D. Minna, M.A. White, GWAS meets TCGA to illuminate mechanisms of cancer predisposition, *Cell*, 152 (2013) 387-389.
- [16] F. Ponten, K. Jirstrom, M. Uhlen, The Human Protein Atlas--a tool for pathology, *The Journal of pathology*, 216 (2008) 387-393.
- [17] Z. Tang, C. Li, B. Kang, G. Gao, C. Li, Z. Zhang, GEPIA: a web server for cancer and normal gene expression profiling and interactive analyses, *Nucleic acids research*, 45 (2017) W98-W102.
- [18] X.B. Huang, C.M. Yang, Q.M. Han, X.J. Ye, W. Lei, W.B. Qian, MNK1 inhibitor CGP57380 overcomes mTOR inhibitor-induced activation of eIF4E: the mechanism of synergic killing of human T-ALL cells, *Acta pharmacologica Sinica*, 39 (2018) 1894-1901.
- [19] W. Wang, Q. Wen, J. Luo, S. Chu, L. Chen, L. Xu, H. Zang, M.M. Alnemah, J. Li, J. Zhou, S. Fan, Suppression Of beta-catenin Nuclear Translocation By CGP57380 Decelerates Poor Progression And Potentiates Radiation-Induced Apoptosis in Nasopharyngeal Carcinoma, *Theranostics*, 7 (2017) 2134-2149.
- [20] Q. Wen, W. Wang, J. Luo, S. Chu, L. Chen, L. Xu, H. Zang, M.M. Alnemah, J. Ma, S. Fan, CGP57380 enhances efficacy of RAD001 in non-small cell lung cancer through abrogating mTOR inhibition-induced phosphorylation of eIF4E and activating mitochondrial apoptotic pathway, *Oncotarget*, 7 (2016) 27787-27801.
- [21] J.K. Altman, A. Szilard, B.W. Konicek, P.W. Iversen, B. Kroczyńska, H. Glaser, A. Sassano, E. Vakana, J.R. Graff, L.C. Plataniias, Inhibition of Mnk kinase activity by cercosporamide and suppressive effects on acute myeloid leukemia precursors, *Blood*, 121 (2013) 3675-3681.
- [22] V.H. Dao, I. Ourliac-Garnier, M.A. Bazin, C. Jacquot, B. Baratte, S. Ruchaud, S. Bach, O. Grovel, P. Le Pape, P. Marchand, Benzofuro[3,2-d]pyrimidines inspired from cercosporamide CaPkc1 inhibitor: Synthesis and evaluation of fluconazole susceptibility restoration, *Bioorganic & medicinal chemistry letters*, 28 (2018) 2250-2255.

- [23] A. Furukawa, T. Arita, T. Fukuzaki, S. Satoh, M. Mori, T. Honda, Y. Matsui, K. Wakabayashi, S. Hayashi, K. Araki, J. Ohsumi, Substituents at the naphthalene C3 position of (-)-Cercosporamide derivatives significantly affect the maximal efficacy as PPAR γ partial agonists, *Bioorganic & medicinal chemistry letters*, 22 (2012) 1348-1351.
- [24] S.H. Reich, P.A. Sprengeler, G.G. Chiang, J.R. Appleman, J. Chen, J. Clarine, B. Eam, J.T. Ernst, Q. Han, V.K. Goel, E.Z.R. Han, V. Huang, I.N.J. Hung, A. Jemison, K.A. Jessen, J. Molter, D. Murphy, M. Neal, G.S. Parker, M. Shaghafi, S. Sperry, J. Staunton, C.R. Stumpf, P.A. Thompson, C. Tran, S.E. Webber, C.J. Wegerski, H. Zheng, K.R. Webster, Structure-based Design of Pyridone-Aminal eFT508 Targeting Dysregulated Translation by Selective Mitogen-activated Protein Kinase Interacting Kinases 1 and 2 (MNK1/2) Inhibition, *Journal of medicinal chemistry*, 61 (2018) 3516-3540.
- [25] B.W. Konicek, A.R. Capen, K.M. Credille, P.J. Ebert, B.L. Falcon, G.L. Heady, B.K.R. Patel, V.L. Peek, J.R. Stephens, J.A. Stewart, S.L. Stout, D.E. Timm, S.L. Um, M.D. Willard, I.H. Wulur, Y. Zeng, Y. Wang, R.A. Walgren, S.C. Betty Yan, Merestinib (LY2801653) inhibits neurotrophic receptor kinase (NTRK) and suppresses growth of NTRK fusion bearing tumors, *Oncotarget*, 9 (2018) 13796-13806.
- [26] E.M. Kosciuczuk, D. Saleiro, B. Kroczyńska, E.M. Beauchamp, F. Eckerdt, G.T. Blyth, S.M. Abedin, F.J. Giles, J.K. Altman, L.C. Plataniias, Merestinib blocks Mnk kinase activity in acute myeloid leukemia progenitors and exhibits antileukemic effects in vitro and in vivo, *Blood*, 128 (2016) 410-414.
- [27] S.B. Yan, S.L. Um, V.L. Peek, J.R. Stephens, W. Zeng, B.W. Konicek, L. Liu, J.R. Manro, V. Wacheck, R.A. Walgren, MET-targeting antibody (emibetuzumab) and kinase inhibitor (merestinib) as single agent or in combination in a cancer model bearing MET exon 14 skipping, *Investigational new drugs*, 36 (2018) 536-544.
- [28] Y. Zhan, J. Guo, W. Yang, C. Goncalves, T. Rzymiski, A. Dreas, E. Zylkiewicz, M. Mikulski, K. Brzozka, A. Golas, Y. Kong, M. Ma, F. Huang, B. Huor, Q. Guo, S.D. da Silva, J. Torres, Y. Cai, I. Topisirovic, J. Su, K. Bijian, M.A. Alaoui-Jamali, S. Huang, F. Journe, G.E. Ghanem, W.H. Miller, Jr., S.V. Del Rincon, MNK1/2 inhibition limits oncogenicity and metastasis of KIT-mutant melanoma, *The Journal of clinical investigation*, 127 (2017) 4179-4192.
- [29] X. Jin, J. Merrett, S. Tong, B. Flower, J. Xie, R. Yu, S. Tian, L. Gao, J. Zhao, X. Wang, T. Jiang, C.G. Proud, Design, synthesis and activity of Mnk1 and Mnk2 selective inhibitors containing thieno[2,3-d]pyrimidine scaffold, *European journal of medicinal chemistry*, 162 (2019) 735-751.
- [30] Y. Matsui, I. Yasumatsu, K.I. Yoshida, S. Iimura, Y. Ikeno, T. Nawano, H. Fukano, O. Ubukata, H. Hanzawa, F. Tanzawa, T. Isoyama, A novel inhibitor stabilizes the inactive conformation of MAPK-interacting kinase 1, *Acta crystallographica. Section F, Structural biology communications*, 74 (2018) 156-160.
- [31] G.B. Xu, G. He, H.H. Bai, T. Yang, G.L. Zhang, L.W. Wu, G.Y. Li, Indole Alkaloids from *Chaetomium globosum*, *Journal of Natural Products*, 78 (2015) 1479-1485.
- [32] B.W. Ke, M. Tian, J.J. Li, B. Liu, G. He, Targeting Programmed Cell Death Using Small-Molecule Compounds to Improve Potential Cancer Therapy, *Medicinal Research Reviews*, 36 (2016) 983-1035.
- [33] L. Ouyang, Y. Chen, X.Y. Wang, R.F. Lu, S.Y. Zhang, M. Tian, T. Xie, B. Liu, G. He, *Polygonatum odoratum* lectin induces apoptosis and autophagy via targeting EGFR-mediated

Ras-Raf-MEK-ERK pathway in human MCF-7 breast cancer cells, *Phytomedicine*, 21 (2014) 1658-1665.

[34] B. Han, W. Huang, W. Ren, G. He, J.H. Wang, C. Peng, Asymmetric Synthesis of Cyclohexane-Fused Drug-Like Spirocyclic Scaffolds Containing Six Contiguous Stereogenic Centers via Organocatalytic Cascade Reactions, *Advanced Synthesis & Catalysis*, 357 (2015) 561-568.

[35] G. He, F.B. Wu, W. Huang, R. Zhou, L. Ouyang, B. Han, One-Pot Asymmetric Synthesis of Substituted Tetrahydrofurans via a Multicatalytic Benzoin/Michael/Acetalization Cascade, *Advanced Synthesis & Catalysis*, 356 (2014) 2311-2319.

[36] Q. Li, L. Zhou, X.D. Shen, K.C. Yang, X. Zhang, Q.S. Dai, H.J. Leng, Q.Z. Li, J.L. Li, Stereoselective Construction of Halogenated Quaternary Carbon Centers by Bronsted Base Catalyzed 4+2 Cycloaddition of α -Haloaldehydes, *Angew. Chem.-Int. Edit.*, 57 (2018) 1913-1917.

[37] Y. Chen, Y.X. Zheng, Q.L. Jiang, F.F. Qin, Y.H. Zhang, L.L. Fu, G. He, Integrated bioinformatics, computational and experimental methods to discover novel Raf/extracellular-signal regulated kinase (ERK) dual inhibitors against breast cancer cells, *European journal of medicinal chemistry*, 127 (2017) 997-1011.

[38] Z.P. Pan, Y.J. Chen, J.Y. Liu, Q.L. Jiang, S.Y. Yang, L. Guo, G. He, Design, synthesis, and biological evaluation of polo-like kinase 1/eukaryotic elongation factor 2 kinase (PLK1/EEF2K) dual inhibitors for regulating breast cancer cells apoptosis and autophagy, *European journal of medicinal chemistry*, 144 (2018) 517-528.

[39] M.C. Yang, C. Peng, H. Huang, L. Yang, X.H. He, W. Huang, H.L. Cio, G. He, B. Han, Organocatalytic Asymmetric Synthesis of Spiro-oxindole Piperidine Derivatives That Reduce Cancer Cell Proliferation by Inhibiting MDM2-p53 Interaction, *Organic Letters*, 19 (2017) 6752-6755.

[40] Y.H. Zhang, C.T. Wang, W. Huang, P. Haruehanroengra, C. Peng, J. Sheng, B. Han, G. He, Application of organocatalysis in bioorganometallic chemistry: asymmetric synthesis of multifunctionalized spirocyclic pyrazolone-ferrocene hybrids as novel RalA inhibitors, *Organic Chemistry Frontiers*, 5 (2018) 2229-2233.

[41] Q. Zhao, C. Peng, H. Huang, S.J. Liu, Y.J. Zhong, W. Huang, G. He, B. Han, Asymmetric synthesis of tetrahydroisoquinoline-fused spirooxindoles as Ras- GTP inhibitors that inhibit colon adenocarcinoma cell proliferation and invasion, *Chemical Communications*, 54 (2018) 8359-8362.

[42] Y.J. Chen, F.J. Yuan, X. Jiang, Q. Lv, N. Luo, C.Y. Gong, C.T. Wang, L. Yang, G. He, Discovery of a self-assembling and self-adjuvant lipopeptide as a saccharide-free peptide vaccine targeting EGFRvIII positive cutaneous melanoma, *Biomaterials Science*, 6 (2018) 1120-1128.

[43] X.Y. Wang, F.B. Wu, G.Y. Li, N. Zhang, X.R. Song, Y. Zheng, C.Y. Gong, B. Han, G. He, Lipid-modified cell-penetrating peptide-based self-assembly micelles for co-delivery of narciclasine and siULK1 in hepatocellular carcinoma therapy, *Acta Biomaterialia*, 74 (2018) 414-429.

[44] R. Zhou, Q.J. Wu, M.R. Guo, W. Huang, X.H. He, L. Yang, F. Peng, G. He, B. Han, Organocatalytic cascade reaction for the asymmetric synthesis of novel chroman-fused spirooxindoles that potently inhibit cancer cell proliferation, *Chemical Communications*, 51 (2015) 13113-13116.

Graphical abstract

Design, synthesis and biological evaluation of 4- aniline-thieno[2,3-d]pyrimidine derivatives as MNK1 inhibitors against renal cell carcinoma and nasopharyngeal carcinoma

Min Zhang,^{†,1} Li Jiang,^{†,1} Jia Tao,¹ Zhaoping Pan,² Minyao He,² Dongyuan Su,³ Gu He^{2,*} and Qinglin Jiang^{1,*}

